Electrocatalytic evidence of the diversity of the oxygen reaction in the bacterial bd oxidase from different organisms

Anton Nikolaev, S Safarian, A Thesseling, D Wohlwend, T Friedrich, H Michel, T Kusumoto, J Sakamoto, Frederic Melin, Petra Hellwig

Electrocatalytic evidence of the diversity of the oxygen reaction in the bacterial *bd* oxidase from different organisms

Anton Nikolaev[‡ [a]], Schara Safarian[‡ [b]], Alexander Thesseling[[c]], Daniel Wohlwend [[c],] Thorsten Friedrich[[c]], Hartmut Michel[[b]], Tomoichirou Kusumoto[[d]], Junshi Sakamoto[[d]], Frederic Melin[* [a]], Petra Hellwig[* [a,e]]

[a] Dr. A. Nikolaev, Dr. F. Melin, Prof. Dr. P. Hellwig
Laboratoire de Bioélectrochimie et Spectroscopie, UMR 7140, Chimie de la Matière Complexe,
Université de Strasbourg - CNRS
4, rue Blaise Pascal, 67081 Strasborg, France

E-mail: fmelin@unistra.fr, hellwig@unistra.fr,

[b] Dr. S. Safarian, Prof. Dr. H. Michel
Max Planck Institute of Biophysics, Frankfurt am Main, Germany

[c] Dr. A. Thesseling, Dr. D. Wohlwend, Prof. Dr. T. Friedrich Institut für Biochemie, Albert-Ludwigs-Universität Freiburg, Freiburg, Germany

[d] T. Kusumoto, Prof. Dr. J. Sakamoto Department of Bioscience and Bioinformatics Kyushu Institute of Technology, 680-4 Kawazu, Fukuoka Japan

[e] Prof. P. Hellwig

USIAS, University of Strasbourg Institute for Advanced Studies, Strasbourg, France

Supporting information for this article is given via a link at the end of the document.

Keywords: cytochrome *bd* oxidase • electrocatalysis • oxygen reduction • diversity of enzymatic reactions • bacterial adaptation.

Abstract: Cytochrome *bd* oxidase is a bacterial terminal oxygen reductase that was suggested to enable adaptation to different environments and to confer resistance to stress conditions. An electrocatalytic study of the cyt *bd* oxidases from *Escherichia coli, Corynebacterium glutamicum* and *Geobacillus thermodenitrificans* gives evidence for a different reactivity towards oxygen. An inversion of the redox potential values of the three hemes is found when comparing the enzymes from different bacteria. This inversion can be correlated with different protonated glutamic acids as evidenced by reaction induced FTIR spectroscopy. The influence of the microenvironment of the hemes on the reactivity towards oxygen is discussed.

Introduction

The selective reduction of oxygen to water is crucial to life and a central process in aerobic organisms. It is catalyzed by several different enzymes, including cytochrome *bd* oxidases (cyt *bd*) that are solely present in prokaryotes, including several pathogens such as *Escherichia coli, Mycobacterium tuberculosis* or *Klebsiella pneumoniae* [1-3]. In addition to the reduction of oxygen, they were suggested to play a crucial role in protection against oxidative stress [4, 5], in bacterial virulence [6, 7], adaptability [8] and antibiotics resistance [9, 10]. Understanding their mechanism and physiological role may thus provide insight into bacterial defense strategies.

All known cyt *bd* oxidase enzymes include at least two core transmembrane subunits, CydA and B, binding two B-type hemes and one D-type heme. The reduction of O_2 is suggested to occur at the high spin D-type heme in all cyt *bd* oxidases [3, 11]. Based on the size of the hydrophilic region between transmembrane helices 6 and 7 in CydA, designated as 'Q-loop', these oxidases have been divided into two subfamilies, named ‘L’ and ‘S’ [3]. The L-subfamily includes cyt *bd* from most enterobacterial pathogens that cause infectious diseases, like for example the well-studied cyt *bd*-I enzyme from *E. coli* [12]. The S-subfamily comprises the majority of cyt *bd* but is very little studied. In the *Geobacillus thermodenitrificans* (*G. th*) cyt *bd*, a member of this subfamily, at least two of the hemes have a different structural environment since the heme *d* Q-band in the visible spectra showed a 10 nm shift in comparison to the cyt *bd* of the L-family [13]. In addition, the high-spin heme b_{595} contribution is not evident in visible spectra, as confirmed by CD and MCD spectroscopy [14]. At the same time, other cyt *bd* oxidases from the same subfamily did not show strong shifts in the spectra, pointing towards a large structural diversity. Furthermore, a low sensitivity to CN^- as inhibitor of the active site was reported for some cyt *bd* oxidases [1, 15].

The crystal structure of the *G. th* enzyme [11] and the electron cryo-microscopy (cryo-EM) structures of the *E. coli* enzyme [16, 17] revealed that while both enzymes have a very similar overall architecture, two of the hemes are found in a "switched" position. Residues identified to be crucial for proton translocation are conserved and the loss of a leucine residue in the highly conserved helix between Glu 99 and Glu 107 (*E. coli* numbering is used here) seems to induce the structural rearrangement of the heme ligand that is located at a different distance to the heme (see figure 1). A presentation of the structure of the two enzymes showing the location of all cofactors is available in supporting information (figure S1). Furthermore, an additional single helical subunit is present in the *E coli* cyt *bd* (Cyd H or Y). On the basis of the structural data it was suggested that both enzymes comprise different oxygen pathways [16, 17].

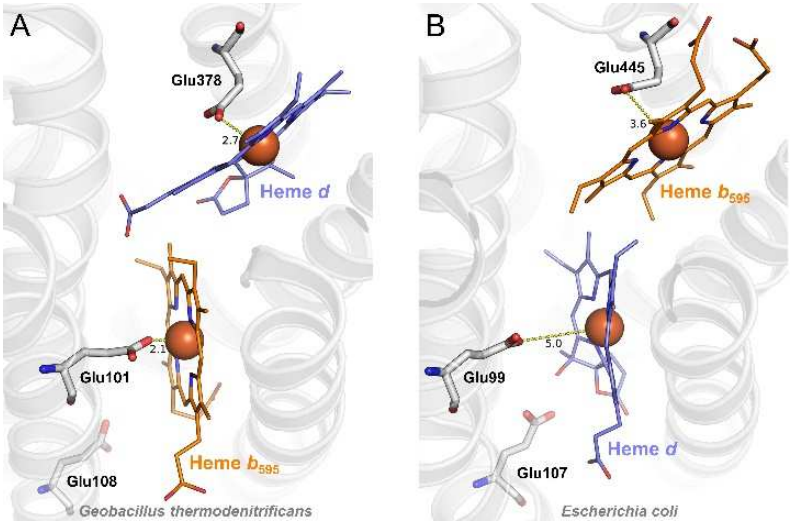

Figure 1. Comparison of the structure from cyt *bd*-I *E. coli* and cyt *bd G. th* (PDB 6RKO and 5DOQ). Three conserved glutamic acid residues are shown.

In this article, we compare the redox potentials and electrocatalytic properties of the cyt *bd* oxidases from *E. coli*, *G. th* and *Corynebacterium glutamicum* (*C. glu*). The differences are discussed in conjunction with the structural and FTIR studies of the enzymes.

Materials and Methods

Protein purification:

G. th cyt *bd* was extracted and purified from membrane fractions of *G. th* K1041/pSTE-*cbdAB* recombinant cells with two consecutive column chromatography of DEAE-Toyopearl and hydroxyapatite in the presence of 0.5%(w/v) MEGA9+10, as described previously [14]. *C. glu* cyt *bd* was extracted and purified from membrane fractions of *C. glu ΔctaD*/pPC4-*cydABDC* recombinant cells [18] with two consecutive chromatography of hydroxyapatite and then DEAE-Toyopearl in the presence of 0.05%(w/v) DDM. The *bd-I* oxidase from *E.coli Δcyo-CydA$_h$BX* strain were prepared as previously described [19]. The protein at final concentration of 10 mg/ml was equilibrated in buffer (20 mM MOPS, 20 mM NaCl, 0.003% MNG, pH 7.0). For the infrared measurements, the cyt *bd* samples have been equilibrated in 50 mM KPi, 100 mM KCl and the respective detergents for each cyt *bd* type (see above).

UV-vis titration

The titrations have been performed using an electrochemical thin layer cell with CaF_2 windows as described previously [20, 21]. A gold grid modified with a 1:1 solution of cysteamine and mercaptopropionic acid was used as working electrode. This mixture of positively and negatively charged thiols served to prevent the adsorption of the protein on the gold surface. A cocktail of 17 mediators was added to the protein sample with a final concentration of 25 µM. A platinum contact was used as counter electrode and an aqueous Ag/AgCl 3 M KCl used as reference electrode. For these experiments, the proteins were

concentrated to approximately 0.4 mM in 20 mM phosphate buffer with 100 mM KCl and 0.05% DDM. The spectra were recorded at 12°C with a Cary 300 spectrometer coupled to a potentiostat. For the oxidative titration, the spectrum at -0.3 V (vs SHE) was taken as reference whereas for the reductive titration, the spectrum at +0.6 V was taken as reference. Spectra were recorded every 25 mV with an equilibration time of at least 20 minutes. The potential was changed when the spectra did not evolve anymore.

Electrocatalytic studies:

The direct electrochemical characterization of the proteins was performed on electrodes modified with gold nanoparticles of 15 nm average diameter, following a procedure already described. The electrodes were modified according to already published procedures [22-24]. Briefly, gold disk electrodes (4.5 mm diameter) were first polished with 0.3μm aluminium oxide powder and then cleaned in 0.1 M H_2SO_4 by cycling electrode potential between −0.15 and +1.7 V vs SHE (100 cycles, 4 V s^{-1}). Three successive aliquots of a solution of 15 nm gold NPs obtained by the procedure of Turkevich et al. [25] and Frens [26] were then deposited on the surface. The gold surface was further modified overnight with a 1 mM solution of 1-hexanethiol and 6-mercapto-hexan-1-ol in ethanol. It is noted that depending on the preparation protocol and concentration of the protein samples, a large excess of detergent is often present in membrane proteins. Prior to adsorption on the electrodes, it was necessary to decrease the amount of detergent by washing 5 μL of the protein sample solution once with 200 μL of potassium phosphate buffer (100 mM, pH 7) devoid of detergent using an Amicon Ultra centrifugal 50 kDa filter. The *E. coli* enzyme was further incubated with 0.025eq of phosphatidylethanolamine, a lipid which is present in the *E. coli* membrane. For *G. th* and *C. glu*, no lipids were added. In each case, 6 μL of protein solution with approximate concentration between 10 and 15 μM were then deposited on the surface of the electrode and

kept at 4◦C for 10 h. The protein excess was removed by rinsing with a 100 mM pH 7 phosphate buffer solution.

All electrochemical experiments were carried out in a 100 mM phosphate buffer solution with a conventional three electrode cell connected to a Versastat 4 potentiostat (Princeton Applied Research, Ametek). A silver chloride electrode (3 M KCl) was used as reference electrode and a platinum wire as counter electrode.

Electrochemically induced FTIR difference spectroscopy:

The measurements were carried out in the same thin-layer cell as the one used for UV/Vis titration under anaerobic conditions. IR spectra were measured with a Vertex 70 FTIR spectrometer (Bruker, Germany). Complete reduction and oxidation of the enzyme were obtained at -0.5 V and +0.5 V (vs Ag/AgCl) respectively. Spectra were recorded after an equilibration time of 5 minutes for both oxidation and reduction. For each state, two spectra (256 scans and 4 cm^{-1} resolution) were recorded and averaged. The reaction was typically cycled 40-45 times and the difference spectra averaged. The temperature of the electrochemical cell was fixed at 5°C throughout the experiment. Infrared spectra were humidity and baseline corrected.

Infrared Absorption spectroscopy

For the infrared absorption spectroscopy experiments and analysis of the amide I band of the *G. th* enzyme, the protein was washed in D_2O based buffer either at pD 7 or pD 9.5, because H_2O shows a strong absorption in the Amide I region. 2.5 µL of 10 µM protein solution were deposited between two CaF_2 windows and the spectra were measured using a Bruker Vertex 70 spectrometer with an accumulation of 256 scans at a resolution of 4 cm^{-1}.

Results and Discussion

Redox potentials and electron transfer path.

Most mechanistic and biochemical studies were performed with the cyt *bd*-I from *E. coli*. The enzyme was shown to generate a proton-motive force by taking the four protons required for O_2 reduction from the cytoplasmic side of the membrane and releasing the protons from quinol oxidation to the periplasmic side [27]. Electrons were suggested to be transferred from the donor (ubi- or menaquinol) to heme b_{558} [28], heme b_{595} and finally to the *d*-heme center where oxygen is believed to be reduced [3]. Interestingly, the equilibrium potentials of the hemes in *G. th* cyt *bd* were found to be different from that of the *E coli* enzyme, in line with the different structural arrangement of the heme groups described above (figure 2). Whereas in *E. coli* heme *d* has the highest Em value of all hemes (258 mV, pH7, SHE), in *G. th* a significantly lower value is observed (15 mV, pH7, SHE) [29] (Fig. 2). The *C. glu* cyt *bd* oxidase follows the same order of potentials like the *E coli* enzyme. It is noted that electron transfer is slow in the *C. glu* enzyme and duroquinone needed to be added to obtain the equilibrium potentials that still show a high error of 40 mV (figure 2).

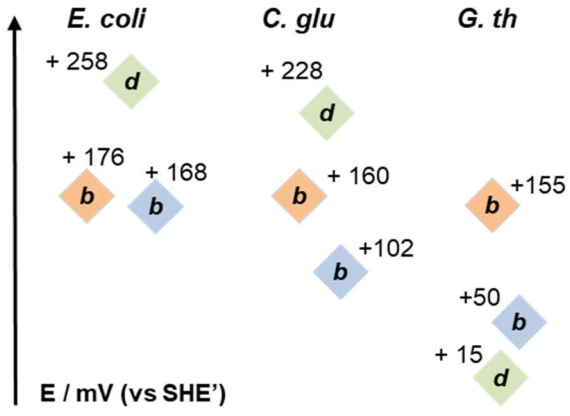

Figure 2. Redox potentials obtained from spectro-electrochemical titrations of cyt *bd* from *G. th*, *C. glu* and *E. coli* at pH 7 (vs SHE'), for methods see [21]. The experimental titration curves are shown in Supporting Information (Figures S2 and S3).

Protein film voltammetry and catalytic reaction with oxygen.

In order to probe the oxygen reactivity of these three different cyt *bd* oxidases, electrocatalytic experiments were performed for the proteins immobilized on gold nanoparticles modified with thiols as described for the *E. coli* enzyme [23, 24]. The gold nanoparticles are used to improve the electron transfer between the electrode and the cofactor of the enzymes [30-33]. For largely hydrophobic proteins such as the cyt *bd* oxidases, we are using a (1/1) mixture of neutral 6-mercaptohexan-1-ol and 1-hexanethiol. The experimental conditions were adapted by optimizing the lipid and detergent content for each enzyme, as described in Materials and Methods. Protein film voltammetry provides insights into the sequence of catalytic events, such as electron transfer and protonation reactions [34-38]. The measured current and its dependence on the electrode potential reveal the enzyme's intrinsic properties.

The electrochemical signatures obtained at the rotating disk electrode in the presence of oxygen with the three *bd* oxidases are shown in Figure 3 for a rotation speed of 1000 r/min. For the *E. coli* cyt *bd* (Fig 3A) a sigmoidal catalytic curve with an $E_{1/2}$ at about 100 mV (vs SHE, pH 7, 23°C) was obtained corresponding to the catalytic reduction of oxygen by the immobilized cyt *bd* oxidase as described before [23, 24].

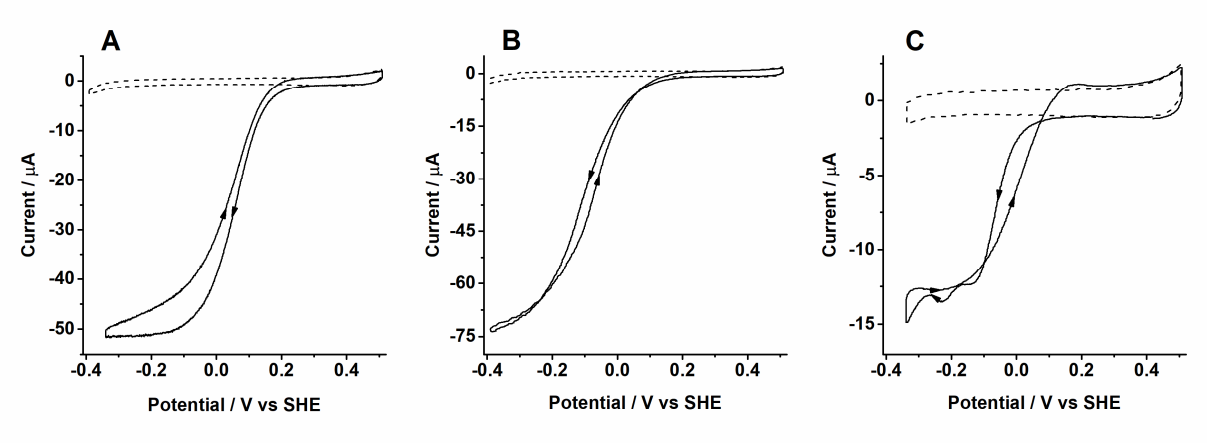

Figure 3. Cyclic voltammograms of cytochrome *bd* oxidases from *E. coli* (A), *C. glu* (B) and *G. th* (C) immobilized on gold NPs. Measurement conditions: pH 7, 25°C, scan rate 0.02 V/s

and rotation rate 1000 rpm. The dash curves show the voltammograms of the modified gold nanoparticles electrodes in the absence of protein.

The electrocatalytic study of cyt *bd* from *C. glu* also reveals a sigmoidal curve with a $E_{1/2}$ at about 0 mV and a crossover of the signal. This crossover shows that the oxygen reduction is more efficient after exposing the protein to reducing potentials, even if the effect is rather small (a few mV only).

Generally, the intensity of the current is proportional to the coverage of the electrode with protein and to the turnover rate. The curve thus describes the relation between the driving force (potential) and the catalytic activity. The amplitude, shape and position of the signals depend on i) oxygen diffusion to and within the enzyme, ii) its binding and reaction at the active site, iii) coupled steps including proton binding and release as well as diffusion of the reaction product and iv) regeneration of the redox state of the active site upon intramolecular electron transfer. The interfacial electron transfer between the electrode and a redox center that is exposed at the protein surface may also play a crucial role [34-39]. Thus there is not necessarily a correlation between the catalytic potential and the redox potential of the active site. The potential at which O_2 reduction takes place with these enzymes is much lower than the redox potential of the *d*-heme.

The electrocatalytic response that was observed for the *G. th* cyt *bd* is characterized by a larger hysteresis and several crossovers during the electrocatalytic measurements. On the forward scan, the onset for the O_2 reduction is several tens of mV more negative than on the reverse scan, revealing that the oxygen reduction is more efficient after the protein has been exposed to reducing potentials. At a value around – 200 mV two inflection points are seen, indicating coupled process. The effect is even more pronounced at 45°C, where the catalytic current is significantly higher (Fig 4). These crossovers and the catalytic potentials are

reproducible for different electrodes and conserved along consecutive cycles (see figures S4-S6 in supporting information).

The increase in intensity at higher temperature is not unusual for thermophilic enzymes and can be correlated with the higher catalytic turnover numbers as described before [40]. A hysteresis within a cyclo-voltammogram was observed for enzymes such as bilirubin oxidase [41] and nitrite reductase [42] and it was attributed to a coupled activation/inactivation process during turnover. This can for example be linked to an inhibition by the substrate, or binding of a ligand like Cl^-. An effect of Cl^-, in the case of the cyt *bd* from *G. th* was excluded (Figure S7). The catalytic events affecting the shape of the curve are often slow in comparison to the electron transfer or the diffusion of the substrates. In cytochrome *c* oxidases that are well known to show a strong cooperative mechanism between the hemes, a 'simple' sigmoidal curve was reported [40, 43, 44] for the oxygen reaction, so cooperative effects between the hemes does not necessarily induce crossovers.

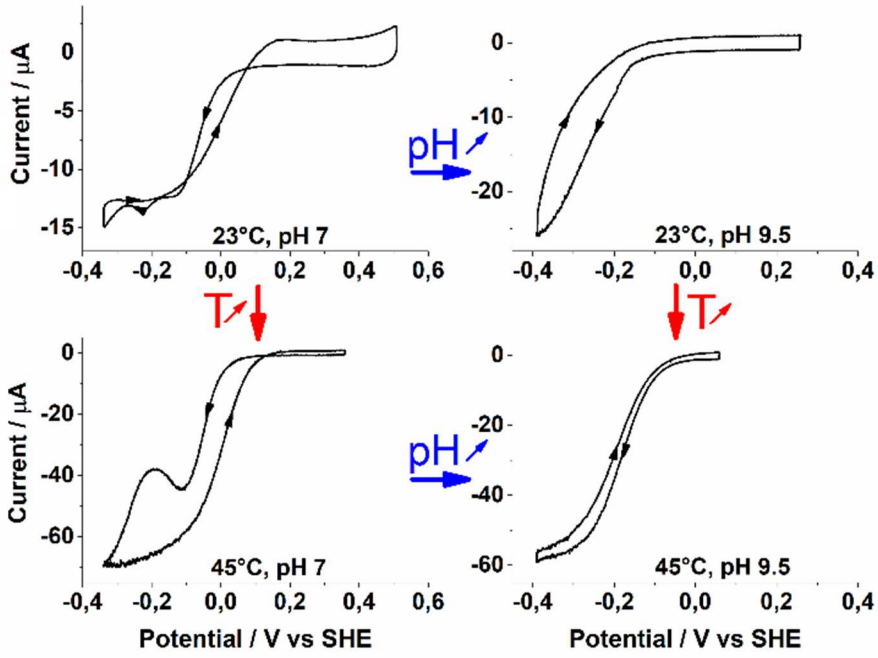

Figure 4. Cyclic voltammograms of cyt *bd* oxidase from *G. th* immobilized on gold NPs under various conditions of temperature and pH. Measurement conditions: scan rate 0.02 V/s and rotation rate 1000 rpm.

pH dependence

Possible coupling process(es) underlying the reaction, have been studied on the basis of the pH dependence of the i = f(E) curve. In Figures 4 and S8, at a pH above 9, and at a T above 40°C, the curves strongly change in shape and become like the one from *E. coli*, however at a lower potential. The proteins are immobilized on gold nanoparticles modified with thiols that remain uncharged over the whole pH range. The protein itself has a largely hydrophobic surface, so it is unlikely that major changes in the interaction between the proteins and the thiol-modified NPs can explain the effect observed here. But it may originate from one (or several) pH dependent reaction steps like for example protonation/deprotonation reactions of amino acid side chains or a pH dependent conformational change of the proteins. A significant change in the heme environment upon pH change could be excluded from the independence of the Vis spectra on the respective pH values (see figure S9). Both cyt *bd* oxidases show the highest activity at a pH around 6.5 [45] and the complex catalytic behavior at pH 7 reflects best the *in vivo* reaction.

A pH and redox dependent conformational change seem to take place for efficient electron and/or proton transfer. This may be the reorganization of a structural element. It is noted that the pH value above 9, where an electrochemical signature without any crossover is seen for the *G. th* cyt *bd*, is not physiological, since the bacteria stop growing at a pH of 8.5.

Redox induced FTIR spectra and the role of protonated acidic residues

Reaction induced FTIR difference spectroscopy is an established technique that allows studying the reorganization in a protein upon an induced reaction. Electrochemically induced difference spectra can be obtained in the same transmission cell used for the redox titrations discussed above [20] and they allow to visualize the contributions that change when switching from an oxidized to a reduced state, or *vice versa*. Typically, contributions from the cofactors (hemes, quinones), the protein backbone and individual amino acids are expected to contribute upon the induced reaction. Importantly, the signals of protonated acidic residues (Asp, Glu) are well known to be distinguished in the spectral range from about 1780 to 1710 cm^{-1}, the exact position depending on the environment of the COOH group [46, 47]. This was also described for cytochrome *c* oxidase [48]. Previous FTIR spectroscopic studies on the cyt *bd* from *E. coli* revealed the presence of signals between 1761, 1751 and 1736 cm^{-1} pointing towards the presence of protonated residues with a pK_a higher than 8 [49]. These signals, that are found at a position typical for a hydrophobic environment are shown in Figure 5Aa. The positive signals can be correlated with the oxidized form of the enzyme and the negative ones with the reduced form. The redox induced FTIR difference spectra of the *C. glu* (Fig 5Ab) and *G. th* (Fig5Ac) cyt *bd* are shown in direct comparison, revealing that in the cyt *bd* from these organisms protonated residues are present under the same conditions. The difference spectra of *C. glu* cyt *bd* are highly comparable to the one from *E. coli*, pointing towards a related environment of these acidic residues. In previous studies on the *E. coli* enzyme, the ν(C=O) of the protonated COOH side chain of E107 (see Fig 5D) was identified to contribute between 1770 and 1750 cm^{-1} [49] and can thus also be expected to be contributing in the case of the *C. glu*. The shape and position of the signals in the *G.th.* cyt *bd* infrared difference spectra is quite different from the *E. coli* and the *C. glu* one. An observation that is in line with the structural differences, where for example the E107 is close to the OH group in the

heme *d* in *E. coli* (see figure 5D), whereas it is close to heme b_{595} in *G. th* (see figure 5B and 5C).

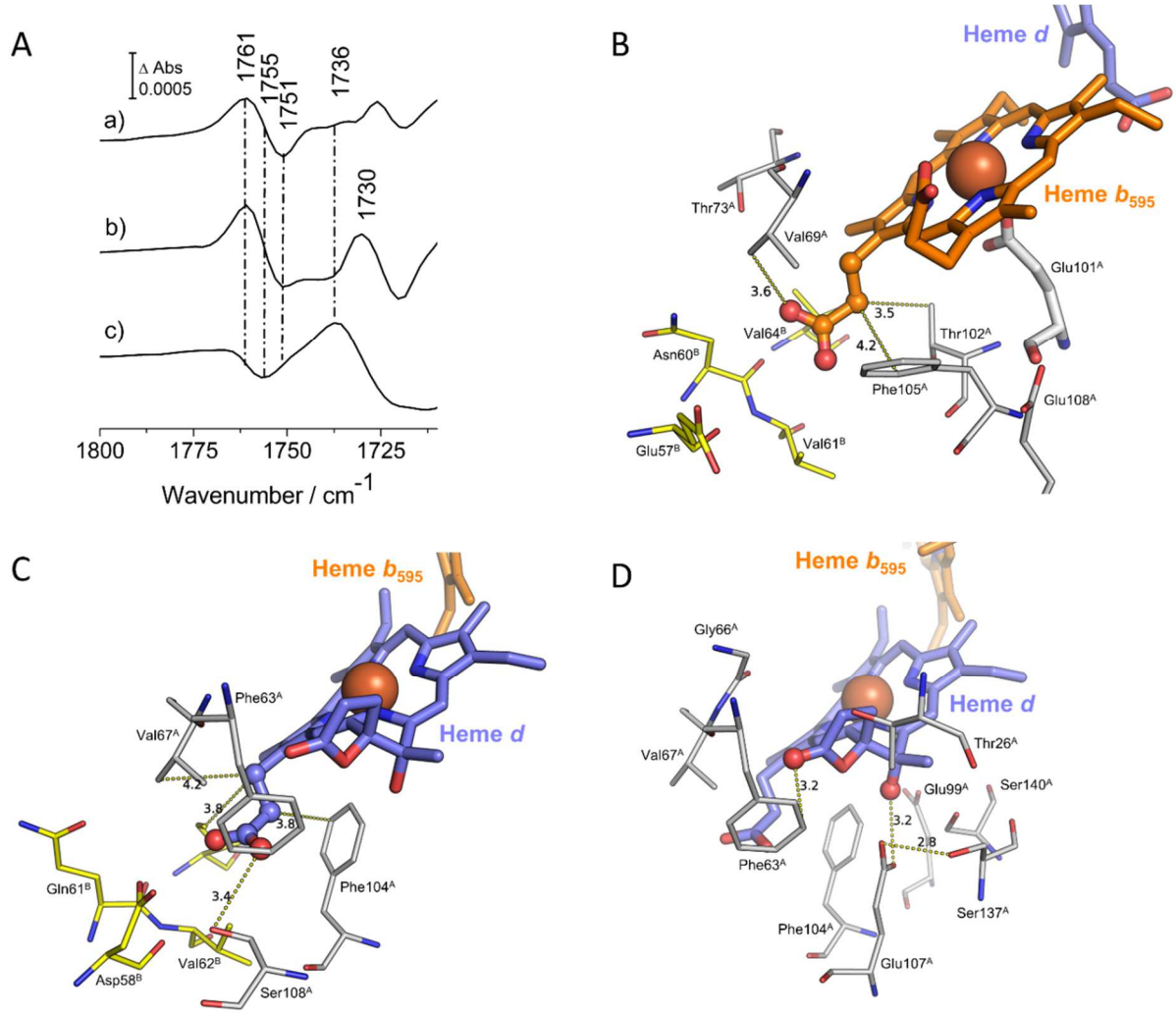

Figure 5. Oxidized-minus-reduced FTIR difference spectra of the cyt *bd* from *E. coli* (a), *C. glu* (b) and *G. th* (c) (A) Comparison of the structure from cyt *bd G. th* 5DOQ (B) and cyt bd-I *E. coli,* PDB 6RKO (C, D).

More specifically in the FTIR difference spectra from *G. th* cyt *bd* the signal at 1760 cm^{-1} is strongly reduced in intensity whereas a strong difference signal at 1736 cm^{-1} is now observed. Also, the smaller signals observed for both, *E. coli* and *C. glu* cyt *bd* have different intensities and positions.

We have probed the electrochemically induced FTIR difference spectra at pH 7 and 9.5 for the *G th.* cyt *bd* in order to identify a possible structural reorganisation upon pH change (see figure S10 and table S1 in supporting information) The very small changes seen excludes a deprotonation reaction, in the spectral region from 1770 – 1710 cm^{-1}, the residues contributing thus have a pK_a higher than 9.5.

In order to probe if the change of reactivity of the cyt *bd* from *G.th* between pH 7 and 9.5 are due to secondary structure alterations, infrared absorption spectra have been measured in the spectral region of the amide I band, seen between 1700 and 1600 cm^{-1} (see figure S11 in supporting information). The analysis is based on contributions of the ν(C=O) vibration of the protein backbone [46, 50, 51]. When comparing the data at pH 7 and 9.5, only some small changes in the shape of the amide I band can be observed and an increased contribution of β-sheets and loops at 1630 and 1680 cm^{-1} point towards a minor structural change of the protein. This structural modification is reversible.

Discussion and conclusion

Previous studies on cyt *bd* from *E. coli* pointed towards close interactions between the three hemes: b_{595}, b_{558} and *d* [21, 52]. For instance, mutations of the highly conserved residue E445 located near heme b_{595}, affected the Raman spectra of heme b_{595} and heme b_{558} [21] and their redox potentials [21, 53]. In the *E. coli* structure, heme b_{595} is located near the periplasmic surface and the heme b_{595} iron is penta-coordinated with E445 as its axial ligand [16]. In the *G. th* cyt *bd*, the change in position of heme b_{595} may explain differences observed in the electrocatalytic curves. Similarly, the conserved residues E107 and E99, that deliver protons to heme *d* in *E. coli* cyt *bd,* are displaced in *G. th* suggesting a different proton path. Importantly the structural data point to a different oxygen/substrate path in the two enzymes (see figure 6) contributing to the different reactivity towards oxygen seen here.

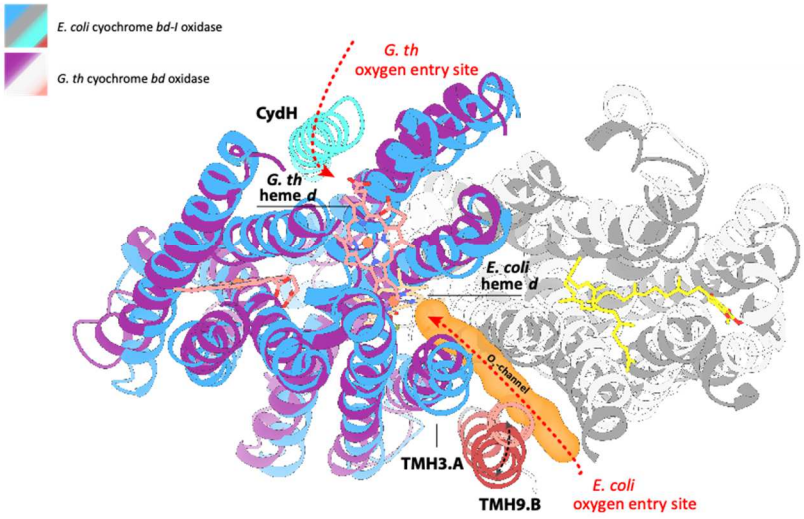

Figure 6. Comparison of the structure from cyt *bd*-I *E. coli* and cyt *bd G. th* PDB 6RKO and 5DOQ.

In previous studies cyt *bd* was found not only to react with O_2 and be part of the bacterial respiratory chains, but also to contribute to the bacterial adaptation to different stress conditions. The enzyme formed complexes with NO, CO or H_2S with a high dissociation rate constant when compared to heme copper oxidases [54, 55]. It was suggested that cyt *bd* confers resistance to NO-stress, and similarly adapts to the other signaling molecules. It is currently hypothesized that the expression of cyt *bd* in pathogenic bacteria may represent a strategy to evade the host immune attack based on production of reactive oxygen species, NO and reactive nitrogen species. These molecules play a major role in human (patho)physiology as signals. It can be expected that bacteria develop the most suitable strategy for their specific environment. This adaption is reflected in the diversity of the electrochemical oxygen reaction together with the structural diversity described here.

Contact and competing interest information for all authors.

The authors declare no competing interests.

Acknowledgements and Funding information

We are indebted to Prof. RB Gennis for valuable discussions on cytochrome *bd* oxidase. PH: ANR-10-LABX-0026_CSC, USIAS-2018-060. JS: Grant-in-Aid for Scientific Research (C) (16K07299). TF: Deutsche Forschungsgemeinschaft by grant *235777276/RTG 1976*. SS: The Nobel laureate Fellowship of the Max Planck Society. HM: Max Planck Society and Deutsche Forschungsgemeinschaft (Cluster of Excellence Macromolecular Complexes).

References

[1] V.B. Borisov, Cytochrome *bd*: Structure and Properties, Biokhimiia 61 (1996) 786-799.
[2] S. Jünemann, Cytochrome *bd* Terminal Oxidase, Biochim. Biophys. Acta, Bioenerg. 1321 (1997) 107-127.
[3] V.B. Borisov, R.B. Gennis, J. Hemp, M.I. Verkhovsky, The Cytochrome *bd* Respiratory Oxygen Reductases, Biochim. Biophys. Acta, Bioenerg. 1807 (2011) 1398-1413.
[4] V.B. Borisov, E. Forte, A. Davletshin, D. Mastronicola, P. Sarti, A. Giuffrè, Cytochrome *bd* Oxidase from *Escherichia coli* Displays High Catalase Activity: an Additional Defense Against Oxidative Stress, FEBS Lett. 587 (2013) 2214-2218.
[5] A. Giuffrè, V.B. Borisov, M. Arese, P. Sarti, E. Forte, Cytochrome *bd* Oxidase and Bacterial Tolerance to Oxidative and Nitrosative Stress, Biochim. Biophys. Acta, Bioenerg. 1837 (2014) 1178-1187.
[6] S.S. Way, S. Sallustio, R.S. Magliozzo, M.B. Goldberg, Impact of either Elevated or Decreased Levels of Cytochrome *bd* Expression on *Shigella flexneri* Virulence, J. Bacteriol. 181 (1999) 1229-1237.
[7] S. Endley, D. McMurray, T.A. Ficht, Interruption of the CydB Locus in *Brucella abortus* Attenuates Intracellular Survival and Virulence in the Mouse Model of Infection, J. Bacteriol. 183 (2001) 2454-2462.
[8] L. Shi, C.D. Sohaskey, B.D. Kana, S. Dawes, R.J. North, V. Mizrahi, M.L. Gennaro, Changes in Energy Metabolism of *Mycobacterium tuberculosis* in Mouse Lung and under *In Vitro* Conditions Affecting Aerobic Respiration, Proc. Natl. Acad. Sci. U. S. A. 102 (2005) 15629-15634.
[9] M. Shepherd, M.E.S. Achard, A. Idris, M. Totsika, M.-D. Phan, K.M. Peters, S. Sarkar, C.A. Ribeiro, L.V. Holyoake, D. Ladakis, G.C. Ulett, M.J. Sweet, R.K. Poole, A.G. McEwan, M.A. Schembri, The Cytochrome *bd-I* Respiratory Oxidase Augments Survival of Multidrug-Resistant *Escherichia coli* During Infection, Sci. Rep. 6 (2016) 35285.
[10] N.P. Kalia, E.J. Hasenoehrl, N.B. Ab Rahman, V.H. Koh, M.L.T. Ang, D.R. Sajorda, K. Hards, G. Grüber, S. Alonso, G.M. Cook, M. Berney, K. Pethe, Exploiting the Synthetic Lethality between Terminal Respiratory Oxidases to Kill *Mycobacterium tuberculosis* and Clear Host Infection, Proc. Natl. Acad. Sci. U. S. A. 114 (2017) 7426-7431.
[11] S. Safarian, C. Rajendran, H. Müller, J. Preu, J.D. Langer, S. Ovchinnikov, T. Hirose, T. Kusumoto, J. Sakamoto, H. Michel, Structure of a *bd* Oxidase Indicates Similar Mechanisms for Membrane-Integrated Oxygen Reductases, Science 352 (2016) 583-586.
[12] M.J. Miller, R.B. Gennis, The Purification and Characterization of the Cytochrome *d* Terminal Oxidase Complex of the *Escherichia coli* Aerobic Respiratory Chain, J. Biol. Chem. 258 (1983) 9159-9165.
[13] J. Sakamoto, E. Koga, T. Mizuta, C. Sato, S. Noguchi, N. Sone, Gene Structure and Quinol Oxidase Activity of a cytochrome *bd*-Type Oxidase from *Bacillus stearothermophilus*, Biochim. Biophys. Acta, Bioenerg. 1411 (1999) 147-158.
[14] A.M. Arutyunyan, J. Sakamoto, M. Inadome, Y. Kabashima, V.B. Borisov, Optical and Magneto-Optical Activity of Cytochrome *bd* from *Geobacillus thermodenitrificans*, Biochim. Biophys. Acta, Bioenerg. 1817 (2012) 2087-2094.
[15] H. Miura, T. Mogi, Y. Ano, C.T. Migita, M. Matsutani, T. Yakushi, K. Kita, K. Matsushita, Cyanide-Insensitive Quinol oxidase (CIO) from *Gluconobacter oxydans* is a Unique Terminal Oxidase Subfamily of Cytochrome *bd*, J. Biochem. 153 (2013) 535-545.
[16] S. Safarian, A. Hahn, D.J. Mills, M. Radloff, M.L. Eisinger, A. Nikolaev, J. Meier-Credo, F. Melin, H. Miyoshi, R.B. Gennis, J. Sakamoto, J.D. Langer, P. Hellwig, W. Kühlbrandt, H. Michel, Active Site Rearrangement and Structural Divergence in Prokaryotic Respiratory Oxidases, Science 366 (2019) 100-104.

[17] A. Theßeling, T. Rasmussen, S. Burschel, D. Wohlwend, J. Kägi, R. Müller, B. Böttcher, T. Friedrich, Homologous *bd* Oxidases Share the Same Architecture but Differ in Mechanism, Nat. Commun. 10 (2019) 5138.
[18] Y. Kabashima, J.-i. Kishikawa, T. Kurokawa, J. Sakamoto, Correlation Between Proton Translocation and Growth: Genetic Analysis of the Respiratory Chain of Corynebacterium glutamicum, The Journal of Biochemistry 146 (2009) 845-855.
[19] A. Theßeling, T. Rasmussen, S. Burschel, D. Wohlwend, J. Kägi, R. Müller, B. Böttcher, T. Friedrich, Homologous *bd* Oxidases Share the Same Architecture but Differ in Mechanism, Nature Commun. 10 (2019) 5138.
[20] D. Moss, E. Nabedryk, J. Breton, W. MÄNtele, Redox-linked conformational changes in proteins detected by a combination of infrared spectroscopy and protein electrochemistry, Eur. J. Biochem. 187 (1990) 565-572.
[21] J. Zhang, P. Hellwig, J.P. Osborne, H.-w. Huang, P. Moënne-Loccoz, A.A. Konstantinov, R.B. Gennis, Site-Directed Mutation of the Highly Conserved Region near the Q-Loop of the Cytochrome bd Quinol Oxidase from Escherichia coli Specifically Perturbs Heme b595, Biochemistry 40 (2001) 8548-8556.
[22] T. Meyer, J. Gross, C. Blanck, M. Schmutz, B. Ludwig, P. Hellwig, F. Melin, Electrochemistry of Cytochrome c1, Cytochrome c552, and CuA from the Respiratory Chain of Thermus thermophilus Immobilized on Gold Nanoparticles, J. Phys. Chem. B 115 (2011) 7165-7170.
[23] E. Fournier, A. Nikolaev, H.R. Nasiri, J. Hoeser, T. Friedrich, P. Hellwig, F. Melin, Creation of a Gold Nanoparticle Based Electrochemical Assay for the Detection of Inhibitors of Bacterial Cytochrome *bd* Oxidases, Bioelectrochemistry 111 (2016) 109-114.
[24] A. Nikolaev, I. Makarchuk, A. Thesseling, J. Hoeser, T. Friedrich, F. Melin, P. Hellwig, Stabilization of the Highly Hydrophobic Membrane Protein, Cytochrome bd Oxidase, on Metallic Surfaces for Direct Electrochemical Studies, Molecules 25 (2020) 3240.
[25] J. Turkevich, P.C. Stevenson, J. Hillier, A Sudy of the Nucleation and Growth Processes in the Synthesis of Colloidal Gold, Discuss. Faraday Soc. 11 (1951) 55-75.
[26] G. Frens, Controlled Nucleation for the Regulation of the Particle Size in Monodisperse Gold Suspensions, Nat. Phys. Sci. 241 (1973) 20-22.
[27] M.J. Miller, R.B. Gennis, The Cytochrome *d* Complex Is a Coupling Site in the Aerobic Respiratory Chain of *Escherichia coli*, J. Biol. Chem. 260 (1985) 14003-14008.
[28] G.N. Green, R.M. Lorence, R.B. Gennis, Specific Overproduction and Purification of the Cytochrome b_{558} Component of the Cytochrome *d* Complex from *Escherichia coli*, Biochemistry 25 (1986) 2309-2314.
[29] I. Belevich, V.B. Borisov, D.A. Bloch, A.A. Konstantinov, M.I. Verkhovsky, Cytochrome *bd* from *Azotobacter vinelandii*: Evidence for High-Affinity Oxygen Binding, Biochemistry 46 (2007) 11177-11184.
[30] Y. Xiao, F. Patolsky, E. Katz, J.F. Hainfeld, I. Willner, "Plugging into Enzymes": Nanowiring of Redox Enzymes by a Gold Nanoparticle, Science 299 (2003) 1877.
[31] I. Griva, J.M. Schnur, N. Lebedev, The Role of Electrode Curvature in Controlling Electron Transfer between the Photosynthetic Reaction Center Protein and Gold Nanoelectrodes, ChemPhysChem 11 (2010) 3589-3591.
[32] J.-N. Chazalviel, P. Allongue, On the Origin of the Efficient Nanoparticle Mediated Electron Transfer across a Self-Assembled Monolayer, Journal of the American Chemical Society 133 (2011) 762-764.
[33] A. Barfidokht, S. Ciampi, E. Luais, N. Darwish, J.J. Gooding, Distance-Dependent Electron Transfer at Passivated Electrodes Decorated by Gold Nanoparticles, Analytical Chemistry 85 (2013) 1073-1080.
[34] F.A. Armstrong, Probing Metalloproteins by Voltammetry, Bioinorganic Chemistry, Springer Berlin Heidelberg, Berlin, Heidelberg, 1990, pp. 137-221.
[35] F.A. Armstrong, H.A. Heering, J. Hirst, Reaction of Complex Metalloproteins Studied by Protein-Film Voltammetry, Chem. Soc. Rev. 26 (1997) 169-179.

[36] F.A. Armstrong, Recent Developments in Dynamic Electrochemical Studies of Adsorbed Enzymes and their Active Sites, Curr. Opin. Chem. Biol. 9 (2005) 110-117.
[37] J.N. Butt, F.A. Armstrong, Voltammetry of Adsorbed Redox Enzymes: Mechanisms in the Potential Dimension, in: O. Hammerich, J. Ulstrup (Eds.), Bioinorganic Electrochemistry, Springer Netherlands, Dordrecht, 2008, pp. 91-128.
[38] C. Léger, P. Bertrand, Direct Electrochemistry of Redox Enzymes as a Tool for Mechanistic Studies, Chem. Rev. 108 (2008) 2379-2438.
[39] C. Léger, F. Lederer, B. Guigliarelli, P. Bertrand, Electron Flow in Multicenter Enzymes: Theory, Applications, and Consequences on the Natural Design of Redox Chains, J. Am. Chem. Soc. 128 (2006) 180-187.
[40] T. Meyer, F. Melin, H. Xie, I. von der Hocht, S.K. Choi, M.R. Noor, H. Michel, R.B. Gennis, T. Soulimane, P. Hellwig, Evidence for Distinct Electron Transfer Processes in Terminal Oxidases from Different Origin by Means of Protein Film Voltammetry, J. Am. Chem. Soc. 136 (2014) 10854-10857.
[41] A. de Poulpiquet, C.H. Kjaergaard, J. Rouhana, I. Mazurenko, P. Infossi, S. Gounel, R. Gadiou, M.T. Giudici-Orticoni, E.I. Solomon, N. Mano, E. Lojou, Mechanism of Chloride Inhibition of Bilirubin Oxidases and Its Dependence on Potential and pH, ACS Catal. 7 (2017) 3916-3923.
[42] P. Bertrand, B. Frangioni, S. Dementin, M. Sabaty, P. Arnoux, B. Guigliarelli, D. Pignol, C. Léger, Effects of Slow Substrate Binding and Release in Redox Enzymes: Theory and Application to Periplasmic Nitrate Reductase, J. Phys. Chem. B 111 (2007) 10300-10311.
[43] F. Melin, H. Xie, T. Meyer, Y.O. Ahn, R.B. Gennis, H. Michel, P. Hellwig, The Unusual Redox Properties of C-Type Oxidases, Biochim. Biophys. Acta, Bioenerg. 1857 (2016) 1892-1899.
[44] F. Melin, P. Hellwig, Redox Properties of the Membrane Proteins from the Respiratory Chain, Chem. Rev. 120 (2020) 10244-10297.
[45] J. Sakamoto., personal communication.
[46] A. Barth, Infrared spectroscopy of proteins, Biochim. Biophys. Acta, Bioenerg. 1767 (2007) 1073-1101.
[47] F. Siebert, W. Mäntele, W. Kreutz, Evidence for the protonation of two internal carboxylic groups during the photocycle of bacteriorhodopsin: Investigation of kinetic infrared spectroscopy, FEBS Lett. 141 (1982) 82-87.
[48] P. Hellwig, J. Behr, C. Ostermeier, O.-M.H. Richter, U. Pfitzner, A. Odenwald, B. Ludwig, H. Michel, W. Mäntele, Involvement of Glutamic Acid 278 in the Redox Reaction of the Cytochrome c Oxidase from Paracoccus denitrificans Investigated by FTIR Spectroscopy, Biochemistry 37 (1998) 7390-7399.
[49] J. Zhang, W. Oettmeier, R.B. Gennis, P. Hellwig, FTIR Spectroscopic Evidence for the Involvement of an Acidic Residue in Quinone Binding in Cytochrome *bd* from *Escherichia coli*, Biochemistry 41 (2002) 4612-4617.
[50] E. Goormaghtigh, J.-M. Ruysschaert, V. Raussens, Evaluation of the Information Content in Infrared Spectra for Protein Secondary Structure Determination, Biophys. J. 90 (2006) 2946-2957.
[51] J. De Meutter, E. Goormaghtigh, Evaluation of protein secondary structure from FTIR spectra improved after partial deuteration, Eur. Biophys. J. (2021).
[52] I. Belevich, V.B. Borisov, J. Zhang, K. Yang, A.A. Konstantinov, R.B. Gennis, M.I. Verkhovsky, Time-Resolved Electrometric and Optical Studies on Cytochrome *bd* Suggest a Mechanism of Electron-Proton Coupling in the Di-Heme Active Site, Proc. Natl. Acad. Sci. U. S. A. 102 (2005) 3657-3662.
[53] R. Murali, R.B. Gennis, Functional Importance of Glutamate-445 and Glutamate-99 in Proton-Coupled Electron Transfer During Oxygen Reduction by Cytochrome *bd* from *Escherichia coli*, Biochim. Biophys. Acta, Bioenerg. 1859 (2018) 577-590.
[54] V.B. Borisov, E. Forte, P. Sarti, M. Brunori, A.A. Konstantinov, A. Giuffrè, Redox Control of Fast Ligand Dissociation from *Escherichia coli* Cytochrome *bd*, Biochem. Biophys. Res. Commun. 355 (2007) 97-102.
[55] A. Giuffrè, V.B. Borisov, D. Mastronicola, P. Sarti, E. Forte, Cytochrome *bd* Oxidase and Nitric Oxide: from Reaction Mechanisms to Bacterial Physiology, FEBS Lett. 586 (2012) 622-629.